Multiple Resonance Effects on Raman Scattering at the Yellow-Exciton Series of Cu_2O

Peter Y. Yu* and Y. R. Shen
Department of Physics, University of California, Berkeley, California 94720, and Inorganic Materials Research Division, Lawrence Berkeley Laboratory, Berkeley, California 94720
(Received 12 November 1973)

We have observed sharp resonance enhancements in some two-phonon Raman modes of Cu_2O around the $n = 2$ to 6 peaks of the yellow-exciton series. We explain the results quantitatively by a theory which allows for multiple resonances in the scattering process.

It is well known that the Raman tensor obtained from the perturbation theory can be written as a sum of terms of the form[1,2]

$$M[(\omega_l \pm \omega_1)(\omega_l \pm \omega_2)\cdots(\omega_l \pm \omega_n)]^{-1} \quad (1)$$

where M stands for the product of matrix elements, ω_l is the incident photon energy, and $\omega_1, \ldots, \omega_n$ contain phonon energies and energies of the intermediate states involved. $n-1$ is the order of the Raman process. So far, most work on resonance Raman scattering (RRS) has considered only cases where one of the energy terms in the denominator of Eq. (1) vanishes.[1-4] Intuitively, one would expect the enhancement in the Raman tensor to be even stronger when two or more energy terms in Eq. (1) vanish simultaneously. We will refer to such cases as multiple resonances. Multiple resonance effects (MRE) have been proposed to explain RRS in a few materials,[5-8] but most of these cases do not allow a quantitative comparison between theory and experiment because of the lack of complete RRS spectra. For example, Martin and Varma[9] can compare only the peak heights of the multi-LO phonon modes in CdS with their "cascade" theory. In this Letter, we report the first RRS at excited states of an exciton, with n as large as 6, and show how the experimental line shape can be quantitatively explained by allowing for MRE in the scattering process.

Before presenting our results on Cu_2O, we give first a summary of its physical properties.[10] Because of inversion symmetry, all electronic and vibrational states of Cu_2O have definite parity.[11] The energy and symmetry of its zone-center phonons have been established by a combination of photoluminescence,[12] infrared,[13] and resonant Raman studies[14,15]: Γ_{25}^- (88 cm^{-1}), Γ_{12}^- (110 cm^{-1}), $\Gamma_{15}^{-(1)}$ (TO, 149 cm^{-1}; LO, 153 cm^{-1}), Γ_2^- (348 cm^{-1}, Γ_{25}^+ (515 cm^{-1}), and $\Gamma_{15}^{-(2)}$ (TO, 640 cm^{-1}; LO, 660 cm^{-1}). The yellow-exciton series of Cu_2O shows up in the absorption spectrum [see Fig. 1(a)] as a series of sharp, asymmetric peaks obeying the Rydberg equation[10]

$$\tilde{\omega}_{n0} = 17\,525 - 786n^{-2}\ cm^{-1} \quad (n = 2, 3, 4, 5). \quad (2)$$

The $1s$ exciton (16399.5 cm^{-1}) is electric-dipole forbidden by selection rule.[11]

Cu_2O has been unique in that its RRS results at the $1s$ yellow exciton[14] and the phonon-assisted absorption edge[15] are well understood and have contributed substantially towards the identification of the observed Raman modes. For example, all the odd-parity zone-center phonons showed strong resonance at the $1s$ exciton while

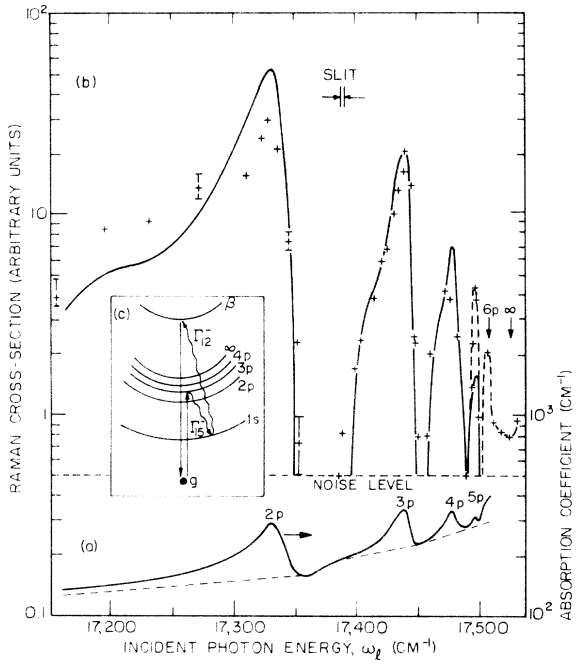

FIG. 1. (a) Absorption spectrum of Cu_2O measured at ~ 5°K. The dashed curve represents the background absorption due to phonon-assisted transitions. (b) Raman cross-section of the $\Gamma_{15}^{-(2)}(LO) + \Gamma_{12}^-(770\ cm^{-1})$ mode of Cu_2O obtained at ~ 10°K as a function of incident photon energies. The solid curve is the theoretical curve [Eq. (6)]. (c) Schematic diagram of the dominant resonant Raman process at $\omega_l \sim \omega_{30}$. g stands for the ground state; β, for an allowed exciton.

two-phonon Raman modes (in which both phonons are odd and one is the Γ_{12}^- mode) showed enhancement at the absorption edge. In addition, we have now observed strong and sharp resonances in several two-phonon modes (involving at least one LO phonon) at the $2p, 3p, \ldots, 6p$ peaks of the yellow exciton. Our RRS results on Cu_2O were obtained at ~10°K with a conventional Raman spectrometer and a cw dye laser tunable between 16 000 and 18 100 cm^{-1}.

Figure 1(b) shows the variation of the Raman cross section of the 770-cm^{-1} $\Gamma_{12}^- + \Gamma_{15}^{-(2)}$(LO) two-phonon mode for ω_l in the region of the yellow excitonic series. This was the *only* mode which showed strong resonances in this region. Figure 2(a) shows a typical Raman spectrum of Cu_2O when ω_l is near an exciton peak.

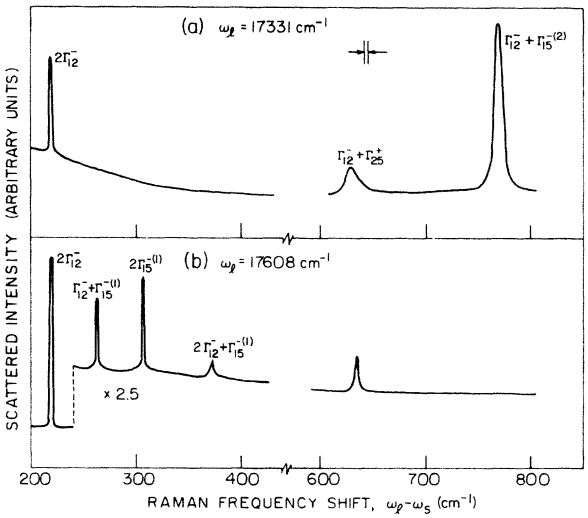

FIG. 2. Raman spectrum of Cu_2O at two different incident photon energies ω_l in the region of the yellow-exciton series: (a) $\omega_l = 17\,331$ and (b) $\omega_l = 17\,608$ cm^{-1}.

To explain these results we have calculated the Raman cross section R by perturbation theory. Among the many possible scattering processes, the one shown in Fig. 1(c) appears to be dominant since it gives the maximum number of resonances (i.e., two) and the strongest exciton-phonon coupling. The Raman cross section, assuming the phonons involved are dispersionless,[16] can be approximated by

$$R(\omega_l) \propto \sum_q \left| \sum_n \frac{M_{g,\beta 0} V^{(12)}_{\beta 0,1\vec{q}} V^{(15)}_{1\vec{q},n0} M_{n0,g}}{(\omega_\beta - \omega_s)(\omega_{1\vec{q}} - \omega_l + \omega(\Gamma_{15}^{-(2)}))(\omega_{n0} - \omega_l)} \right|^2, \tag{3}$$

where M, $V^{(12)}$, and $V^{(15)}$ denote the exciton-photon, exciton-Γ_{12}-phonon, and exciton-$\Gamma_{15}^{-(2)}$-phonon interactions, respectively, and the subscripts represent the various electronic states shown in Fig. 1(c). In Eq. (3) we have neglected the nonresonant background contribution.

It has been shown that[15]

$$M_{g,\beta 0} V^{(12)}_{\beta 0,1\vec{q}} / (\omega_\beta - \omega_s)$$

can be approximated by a constant and

$$|\omega_{1\vec{q}} - \omega|^{-2} \approx [\delta(\omega_{10} + q^2/2\mu - \omega)\pi]/\gamma_1(\vec{q}), \tag{4}$$

where γ_1 is the damping constant of the 1s exciton with wave vector $\vec{q}$. Using these results, we can reduce Eq. (3) to

$$R(\omega_l) \propto \frac{x^{1/2}}{\gamma(x)} \left| \sum_n \frac{f_n(x) M_{n0,g}}{\omega_{n0} - \omega_l} \right|^2, \tag{5}$$

where $x = \omega_{10} - \omega_l + \omega(\Gamma_{15}^{-(2)})$ and $f_n(x)$ comes from the frequency dependence of $V^{(15)}_{1\vec{q},n0}$. When ω varies over only a narrow region around ω_{n0}, the dispersion of $x^{1/2} f_n(x)/\gamma(x)$ can be neglected. Taking into account the damping γ_n of the nth exciton state and neglecting overlap of adjacent exciton peaks, we obtain for $\omega_l \approx \omega_{n0}$,

$$R(\omega_l) = A_n \gamma_n^{-1} \alpha_n(\omega_l), \tag{6}$$

where $\alpha_n(\omega_l)$ is the absorption coefficient of the nth exciton peak in the yellow series and A_n is nearly independent of ω_l. Figure 1(a) shows the absorption spectrum of our Cu_2O sample. It agrees well with previous measurements.[10,17] We obtain $\alpha_n(\omega_l)$ by simply removing the background absorption due to phonon-assisted transitions in the same way as done by Nikitine, Grun, and Sieskind.[18] The dependence of A_n on n can be calculated using the hydrogenic wave functions and assuming $V^{(15)}$ to be given by the Fröhlich interaction.[2] γ_n is estimated from the experimental linewidth of α_n. $R(\omega_l)$ thus obtained is plotted as the solid curve in Fig. 1(b) with only *one* normalization constant. It is seen that agreement with experiment is fairly good. Part of the discrepancy in the fit is due to (1) uncertainty in removing the background absorption and (2) neglect of overlap of neighboring exciton peaks for $n \geq 4$.

On the basis of Fig. 1(c), it is possible to understand the absence of resonance enhancement in

the other two-phonon modes. It is known that LO phonons couple strongly to excitons via the Fröhlich interaction and in Cu_2O only Γ_{12}^- couples the yellow exciton strongly to the β (allowed) excitons. Of the two possible LO phonons, $\Gamma_{15}^{-(2)}$ has a much stronger dipole moment[13,19] and an energy more closely matching the separation of the 1*s* exciton from the higher exciton states than does $\Gamma_{15}^{-(1)}$. It should be pointed out that the strong resonant interband coupling between the 1*s* and 2*p* exciton states via the $\Gamma_{15}^{-(2)}$(LO) phonon can probably explain the large linewidth of the 2*p* exciton peaks.[20]

Although the $\Gamma_{12}^- + \Gamma_{15}^{-(2)}$(LO) mode was the only one to show clear enhancement at the yellow-exciton series, we found that two other two-phonon modes $2\Gamma_{15}^{-(1)}$(LO) (308 cm^{-1}) and $\Gamma_{15}^{-(1)}(LO) + \Gamma_{12}^-$ (264 cm^{-1}), in addition to the $\Gamma_{12}^- + \Gamma_{15}^{-(2)}$(LO) mode, showed strong enhancement when their *scattered* photon frequencies ω_s were resonant with the yellow-exciton series [see Fig. 2(b)]. [We did not study the $2\Gamma_{15}^{-(2)}$(LO) mode because the required ω_l is outside the tuning range of our dye laser.] The dependence of their Raman cross sections on ω_s is shown in Fig. 3(a). Again, detailed considerations led us to conclude that the dominant contributions to the strong enhancements we observed come from MRE (in this case, triple resonances).

As an example, we consider the $2\Gamma_{15}^{-(1)}$(LO) mode since all the exciton-phonon matrix elements can be calculated in this case. For ω_s in resonance with the 2*p* exciton, the dominant scattering process is that shown in Fig. 3(b). Again using perturbation theory, we obtain the Raman cross section for $\omega_s \sim \omega_{20}$ as

$$R(\omega_l) \approx 0 \text{ for } \omega_l - \omega(\Gamma_{15}^{-(1)}) - \omega_{30} < 0, \quad (7a)$$

$$R(\omega_l) \propto [\omega_l - \omega(\Gamma_{15}^{-(1)}) - \omega_{30}]^{1/2} \alpha(\omega_s)/\gamma_3\gamma_2 \quad (7b)$$

otherwise.

Similar expressions are obtained for ω_s in resonance with the higher excitons. The theoretical results are shown as solid curves in Fig. 3(a) where the peak heights have been normalized to the experiment. Again there is good agreement between theory and experiment. Note that the resonance of $\omega_l - \omega(\Gamma_{15}^{-(1)})$ with the $n = 3$ exciton states gave rise to the $[\omega_l - \omega(\Gamma_{15}^{-(1)}) - \omega_{30}]^{1/2}$ term in Eq. (7b). The fact that Eqs. (7) can reproduce the sharp drop in the experimental $R(\omega_l)$ at $\omega_l - \omega(\Gamma_{15}^{-(1)}) - \omega_{30} = 0$ gives strong support to our theory. The details of our theoretical calculations will appear in a later publication.

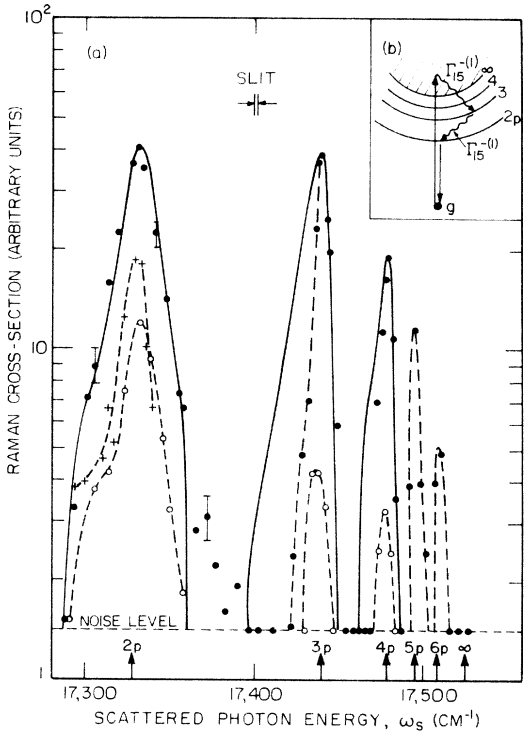

FIG. 3. (a) Raman cross section of three two-phonon modes of Cu_2O measured at ~ 10°K as a function of the *scattered* phonon energy. Closed circles, $2\Gamma_{15}^{-(1)}$(LO) (308 cm^{-1}); open circles, $\Gamma_{12}^- + \Gamma_{15}^{-(1)}$(LO) (264 cm^{-1}); crosses, $\Gamma_{12}^- + \Gamma_{15}^{-(2)}$(LO) (770 cm^{-1}). The solid curve is the theoretical curve. (b) Schematic representation of the Raman process responsible for the observed enhancement in the $2\Gamma_{15}^{-(1)}$(LO) mode at $\omega_s \sim \omega_{20}$.

We also note that the 308-cm^{-1} mode has been observed in photoluminescence[12] and RRS of Cu_2O in the region of the blue and indigo excitons.[21] However, these measurements were not capable of determining whether this mode is a $2\Gamma_{15}^{-(1)}$ or a $2\Gamma_{12}^- + \Gamma_{25}^-$ mode. Our result now shows that the 308-cm^{-1} Raman line is definitely a $2\Gamma_{15}^{-(1)}$(LO) mode.

It should be pointed out that Eqs. (6) and (7) can also be obtained by considering the resonant Raman process as a "cascade"[9] of hot luminescences.[22] For example, in Fig. 3(c) one can consider the scattering process as due to optical excitation of an exciton which then cascades down to the 2*p* level with emission of two $\Gamma_{15}^{-(1)}$(LO) phonons before returning to the ground state with the emission of the scattered photon. But since we have not observed luminescence from excited states of the yellow exciton,[23] we have considered these cases as examples of MRE in RRS rather than hot luminescence. The distinction

between RRS and hot luminescence has been recently elucidated by Shen.[24]

We are grateful to Professor D. Trivich and Professor Y. Petroff for providing the Cu_2O crystals used in our experiment and to Professor L. Falicov for many enlightening discussions. This research was performed under asupices of the U. S. Atomic Energy Commission.

*Present address: Thomas J. Watson Research Center, P. O. Box 218, Yorktown Heights, N.Y. 10598.

[1]R. Loudon, Proc. Roy. Soc., Ser. A 275, 218 (1963), and J. Phys. Radium 26, 677 (1965).

[2]A. K. Ganguly and J. L. Birman, Phys. Rev. 162, 806 (1967).

[3]B. Bendow and J. L. Birman, Phys. Rev. B 1, 1678 (1970), and 4, 569 (1971).

[4]See, for example, J. F. Scott, R. C. C. Leite, and T. C. Damen, Phys. Rev. 188, 1285 (1969).

[5]P. Y. Yu and Y. R. Shen, Phys. Rev. Lett. 29, 468 (1972).

[6]Y. Petroff, P. Y. Yu, and Y. R. Shen, unpublished, and Bull. Amer. Phys. Soc. 18, 413 (1973).

[7]E. F. Gross, A. G. Plyukhin, L. G. Suslina, and E. B. Shadrin, Pis'ma Zh. Eksp. Teor. Fiz. 15, 312 (1972) [JETP Lett. 15, 220 (1972)].

[8]R. C. C. Leite, J. F. Scott, and T. C. Damen, Phys. Rev. Lett. 22, 780 (1969); M. V. Klein and S. P. S. Porto, Phys. Rev. Lett. 22, 782 (1969).

[9]R. M. Martin and C. M. Varma, Phys. Rev. Lett. 26, 1241 (1971).

[10]See, for example, review articles by S. Nikitine, in *Optical Properties of Solids*, edited by S. Nudelman and S. S. Mitra (Plenum, New York, 1969); and by E. F. Gross, Usp. Fiz. Nauk 63, 576 (1957) [Sov. Phys. Usp. 63, 782 (1957)].

[11]R. J. Elliot, Phys. Rev. 124, 340 (1961).

[12]Y. Petroff, P. Y. Yu, and Y. R. Shen, Phys. Rev. Lett. 29, 1558 (1972); A. Compaan and H. Z. Cummins, Phys. Rev. B 6, 4753 (1972).

[13]M. O'Keeffe, J. Chem. Phys. 39, 1789 (1963); I. Pastrniak, Opt. Spektrosk. 6, 107 (1959) [Opt. Spectrosc. 6, 64 (1959)]; J. C. W. Taylor and F. L. Weichman, Can. J. Phys. 49, 601 (1971).

[14]A. Compaan and H. Z. Cummins, Phys. Rev. Lett. 31, 41 (1973).

[15]P. Y. Yu, Y. R. Shen, Y. Petroff, and L. M. Falicov, Phys. Rev. Lett. 30, 283 (1973).

[16]C. Carabatos and B. Perot, Phys. Status Solidi 44, 70 (1971).

[17]P. W. Baumeister, Phys. Rev. 121, 359 (1961).

[18]S. Nikitine, J. B. Grun, and M. Sieskind, J. Phys. Chem. Solids 17, 292 (1961).

[19]K. Huang, Z. Phys. 171, 213 (1963).

[20]Y. Toyozawa, J. Phys. Chem. Solids 25, 59 (1964).

[21]P. Y. Yu, Y. R. Shen, and Y. Petroff, Solid State Commun. 12, 973 (1973).

[22]M. V. Klein, Phys. Rev. B 6, 919 (1973).

[23]Luminescence from excited states of the yellow exciton has been observed by A. Compaan and H. Z. Cummins, Phys. Rev. B 6, 4753 (1972).

[24]Y. R. Shen, Phys. Rev. B (to be published).

Pseudo-One-Dimensional Conductor—Plastically Deformed CdS†

C. Elbaum

Department of Physics and Metals Research Laboratory, Brown University, Providence, Rhode Island 02912

(Received 10 December 1973)

Extraordinary anisotropy (10^8) and unusual temperature dependence of the electrical conductivity have been observed in plastically deformed CdS. These features are attributed to metallic-type conductivity along a pseudo-one-dimensional system consisting of arrays of dislocations. The observed temperature dependence of the conductivity is consistent with a Peierls-type metal-semiconductor transition at 125 K.

Extraordinary anisotropy and unusual temperature dependence of the electrical conductivity of plastically deformed single crystals of CdS (hexagonal) are reported. The observed features are attributed to metallic-type conductivity in a pseudo-one-dimensional system consisting of arrays of dislocations. This interpretation of the experimental results is related to earlier work[1] in which the general problem of electronic energy states of dislocations in compound semiconductors was discussed in some detail.

The experiments are carried out on single crystals of CdS with a room-temperature (298 K) electrical conductivity (in the dark) of $\sim 10^{-6}$ $(\Omega\ \mathrm{cm})^{-1}$; the concentration and type of impurities are not known. Specimens in the shape of rectangular parallelepipeds are prepared with approximate dimensions $3\times4\times5$ mm^3 along directions designated respectively by x, y, and z. The longest (z) and intermediate (y) directions are parallel, respectively, to the $[21\bar{3}0]$ and $[0001]$ crystallographic directions. These specimens are de-